Journal of Sound and Vibration (1998) **218**(1), 1–27
Article No. sv981783

EXACT ADJUSTMENT OF DYNAMIC FORCES IN PRESENCE OF NON-LINEAR FEEDBACK AND SINGULARITY—THEORY AND ALGORITHM

I. BUCHER

Technion, *Faculty of Mechanical Engineering*, *Haifa* 32000, *Israel*

(*Received* 21 *November* 1997, *and in final form* 11 *May* 1998)

This paper describes the theory and algorithm allowing one to tune a multi-exciter system in order to obtain specified temporal and spatial structural response properties. Considerable effort is being put upon the desire to overcome practical difficulties and limitations as found in real-world systems. The main application that was envisaged for this algorithm is the creation of travelling vibration waves in structures. Such waves may be useful in testing and diagnostic applications or in ultrasonic motors for generating motion. The proposed method adaptively modifies a set of perturbations applied to the model so that an increasing amount of information is extracted from the system. The algorithm strives to overcome the following difficulties: (a) singular model inversion, (b) poor signal to noise ratio, (c) feedback, and (d) certain types of non-linear behaviour. High response levels, exciter–structure coupling and the inherent feedback existing in electro-mechanical systems are demonstrated to cause singularity, poor signal to noise levels and, to some extent, non-linear behaviour. These phenomena pose some difficulties under operating conditions commonly encountered during dynamic testing of structures. The tuning of the multi-shaker system is approached in this work, as a non-linear optimisation problem where insight into the physical behaviour is emphasised in choosing the algorithmic strategy. The system's unknown model is inverted in an implicit manner using an automatic orthogonal and adaptive search direction. This adaptation uses the measured responses and forces at each step in order to determine the direction of progression during the tuning process. The non-linear behaviour of the exciters is compensated, in this work, by identification of the high-order (Volterra-like) transfer functions. This high-order model is then inverted allowing one to create a signal that cancels the unwanted harmonics. The proposed approach is analytically shown to converge and the necessary magnitude of perturbations to assure this convergence is derived. A simple case study is used to illustrate the proposed method, while an experimental verification and more examples can be found in a companion paper.

1. INTRODUCTION

The simulation of real-world phenomena in a controlled laboratory experiment is a very desirable goal. This goal is pursued in dynamic testing of structures, where it is required to replicate the time-history of the force patterns being applied in reality. Unfortunately, the exact generation of forcing functions can be very difficult and usually one settles for being able to measure the actually applied

0022–460X/98/460001 + 27 $30.00/0

forces. There are several applications which require precise specification of forces: (a) selective excitation of the structural response for improving the quality of the measured information [1]; (b) stimulating forward or backward whirl in a rotating system [2]; (c) excitation of travelling and standing waves [3]; (d) diagnostics and fault detection [4]; (e) exact replication of measured conditions [5].

Accurate tuning of the forcing functions is essential in all the above mentioned cases and is rewarded in terms of some enhanced (sought) features and by suppression of (unwanted, contaminating) others [3, 6, 7].

The actual force pattern acting upon a vibrating structure is related to both the driving signal provided and the structural response [8]. Due to the dependency of the applied forces on the structural dynamic properties, a very accurate local model of the structure is essential for computing the required driving signals. Such accuracy cannot be achieved when a model is experimentally obtained by means of broad bandwidth measurements (the usual uncertainty in measured modal damping is equal to the estimate itself).

The current problem is related to the estimation of an applied force from the measured response [9] and can thus be classified as an inverse problem [10]. Inverse problems are often more difficult (in some cases a unique solution is unobtainable) to solve and are very sensitive to added noise and model mismatch.

It is well known that the tuning of dynamic force patterns is an iterative process [6], in particular when electro-dynamic shakers are being used. Iterations are required due to the uncertain dynamical behaviour of the combined exciter–structure system and due to the non-linear behaviour of some components in the force path. It has been shown [8] that, in some cases, the applied force depends upon the structural response, thus, in effect a feedback loop that couples the shakers through the response exists. This feedback coupling results in deterioration in the signal to noise ratio and consequently an estimate of the frequency-response function will be biased [8].

When one attempts to exactly tune the applied forces close to resonance conditions, any small deviation in the measurements and consequently the applied force may result in excess motion and hence damage the measurement equipment or the structure. The need for a robust tuning strategy adjusting the external forces in order to assure that those will not exceed an allowable limit is obvious.

Forces are tuned when the classical mode-appropriation technique is exercised. This method is one of the very first modal-testing techniques [11] attributed to Escher. This method, which is still widely used in the aircraft industry, has many limitations and it assumes that perfectly linear structures are dealt with. In this approach any non-linear effect of the forcing system is filtered out (ignored, mostly using tracking filters) and thus are not considered at all. Active control methods applied to structures in general and to rotating machinery in particular lack the precision provided by off-line (or adaptive feed-forward) steady state based methods. This lack of accuracy is mainly due to the constant adaptation of the command signals [6], which is mostly done by means of a steepest-decent type of algorithm. This inaccuracy is attributed to the large condition number (near singularity) of the frequency response matrix combined with periodic and random disturbances existing in rotating machines and to some degree to the non-linearity

existing in all vibrating structures [12]. In order to achieve precise tuning of the response and excitation forces, an off-line iterative method is required. Methods that use non-parametric identification [6] were shown to be successful with a single exciter but this approach lacks the precision a parametric-identification based method has (given the correct parameterisation). When such a non-parametric method is used to cancel non-linear effects, a non-realistic amount of computational effort may be required.

The current paper describes a non-linear optimisation based approach divided into several stages. In the first stage, a specially adapted equation-solver [13, 14] is used and in a later stage a novel scheme exploiting adaptive perturbations motivated by a linearised-model optimisation technique [15] is adopted so that fast convergence and high accuracy are maintained. The proposed algorithm is developed for tuning the amplitude and phase of a multi-shaker sine exciter system and is suitable for tuning either the dynamic forces or the response taking into account a certain type of non-linearity in the vibrating structure. The type of structures considered in this work could be modelled as a polynomial (truncated Volterra) model [16]. The case of rotating machinery is also partly covered by the current method; in these systems the structure is assumed to vibrate due to other effects apart from the applied forces. Non-linear structural identification is an area where much analytical work is shown where the theories of Volterra and Winner [16–21] prevail. On the other hand, no work attempts to identify a non-linear model having several degrees of freedom. Partial identification of non-linear systems is used here where a model has a limited set of frequencies, in a manner similar to reference [16]. This partiality is achieved when harmonic excitation takes place and the work reported in reference [18] has given some motivation for what is done in this work.

The paper is structured as follows. In section 2 the problem at hand is mathematically formulated and a descriptive explanation of the problem follows. Section 3 analyses physical effects making this problem hard to solve where singularity, cross coupling and non-linearity are dealt with separately. In section 4, the proposed tuning and identification algorithm is derived in detail, analysed and compared to the traditional approach. A companion paper provides simulated and experimental evidence for the success of the proposed algorithm, illustrating the benefits of using the proposed approach via case studies. In this work only a brief example showing a simulated case is discussed.

2. DEFINITION OF THE PROBLEM

In this section the problem to be solved is mathematically formulated. A descriptive definition of the problem is provided and the anticipated sources of difficulty are outlined. The practical configuration of a typical system with multiple exciters is illustrated and the feedback, interaction and non-linear behaviour are explained in physical and mathematical terms. It is shown that like most real-world problems, the solution involves a succession of sub-problems, which individually require a thorough understanding of the dynamic characteristics and the physical behaviour dealt with.

2.1. MATHEMATICAL STATEMENT OF THE PROBLEM

The problem is defined for a vibrating structure described by means of a descretised linear equation of motion:

$$\Omega: \quad \mathbf{M}\ddot{\mathbf{x}}(t) + \mathbf{C}\dot{\mathbf{x}}(t) + \mathbf{K}\mathbf{x}(t) = \mathbf{u}(t), \qquad \mathbf{M}, \mathbf{C}, \mathbf{K} \in \Re^{N \times N},$$
$$\mathbf{x}(t), \mathbf{u}(t) \in \Re^{N \times 1}. \tag{1}$$

Here $\mathbf{u}$ incorporates the effect of a set of $\mathbf{P}$ exciters. Those comply with the following non-linear equations:

$$\mathbf{u}(t) = \sum_{k=1}^{NH} \mathbf{F}_k(\boldsymbol{\theta}(\mathbf{v}, t), t) = \sum_{k=1}^{P} \mathbf{K}_k(\mathbf{x}(t)) + \mathbf{d}(t), \tag{2}$$

where $\mathbf{F}_k(\cdot, \cdot)$ is the direct force vector due to the kth shaker, $\boldsymbol{\theta}(\mathbf{v}, t)$ is the vector of the observed parameters (functions), $\mathbf{v} = \mathbf{v}(t)$ is a vector of input signals (controlled inputs), $\mathbf{K}_k(\mathbf{x}(t))$ is a response-related (feedback), (also see below), and $\mathbf{d}(t)$ is the force due to unmeasurable external disturbances.

The response related force (feedback term) has a pronounced effect when high amplitudes of vibration are encountered. $\mathbf{K}_k(\mathbf{x}(t))$ is a symbolic expression for a mathematical operator depending upon the source of feedback. The most common source for a motion related force (feedback) is the back-electro motive force (EMF) observed while using an electro-dynamic actuator. This effect counteracts the desired force (the EMF opposes the currents induced in the shaker) when the excitation frequency is close to resonance and is a strong function of the vibration amplitude.

For the system described in equation (1) the following problem is sought to be solved.

Problem 1: tune forces

Given an elastic structure described by equation (1) and given forcing vectors described by equation (2), and provided that the structural parameters ($\mathbf{M}$, $\mathbf{C}$, $\mathbf{K}$ and $\mathbf{F}_k(\cdot, \cdot)$, $\mathbf{K}_k(\mathbf{x}(t))$) are unknown, then *find* a vector of controlled signals—$\mathbf{v}(t)$, such that the vector of measured forces $\mathbf{u}(t)$ is close, in terms of a distance function $\mathbf{J}(\mathbf{u}(t), \mathbf{u}_d(t))$, to a vector of desired forces $\mathbf{u}_d(t)$.

Mathematically a solution for:

$$\mathbf{v}(t) = \arg\min_{\mathbf{v}(t) \in V} \mathbf{J}(\mathbf{u}(t), \mathbf{u}_d(t)), \tag{3}$$

is sought where V is the set of admissible solution vector functions (of time).

Remark. A similar problem can be stated for tuning the response, in this case $\mathbf{x}(t)$ replaces $\mathbf{u}(t)$ and $\mathbf{x}_d(t)$ replaces $\mathbf{u}_d(t)$ in equation (3).

Problem 1 is very difficult to solve practically using the current state of the art of non-linear systems identification algorithms especially, due to the large number of parameters involved.

Indeed the solution of this problem necessitates a complete identification of the non-linear functional relationship between the excitation $\mathbf{u}(t)$ and the driving signal $\mathbf{v}(t)$ (input voltage). Furthermore, implicit identification of the excited

structure Ω (see equation (1)) is necessary as it enters the functional relation of $\mathbf{u}(t)$ in $\mathbf{v}(t)$ indirectly. In some applications, the external disturbance $\mathbf{d}(t)$ need (can) also be identified and counter-acted (e.g., active cancellation of unbalance in rotating machines).

In this paper, a simpler problem to the one stated above is being solved. For the sake of simplicity and in order to be able to realise the developed algorithms in practice, the dependency of the parameters θ upon time is dropped, but the driving signal $\mathbf{v}(t)$ remains a function of time. The last case represents, for example, steady state or periodic operation.

Problem 2: tune forces: time-independent parameters

This problem is identical to problem 1 with the following parameterisation for the desired excitation and input signals:

$$\mathbf{u}(\boldsymbol{\theta}, t) = \sum_{n=1}^{n_p} \hat{\mathbf{g}}_n(\boldsymbol{\theta}, t), \qquad \mathbf{v}(t) = \mathbf{v}(\rho, t) = \sum_{n=1}^{n_\theta} \hat{\mathbf{g}}_n(\boldsymbol{\rho}, t). \tag{4a}$$

As is evident from equations (4, 4a) the same basis functions $\hat{\mathbf{g}}_n(\cdot, \cdot)$ are being used for representing both the input signals and the resulted force (or response). This allows one to relate more easily the input signal to the tuned quantity (force).

It is further assumed that there is a one-to-one correspondence between $\mathbf{u}(\boldsymbol{\theta}, t)$ and $\boldsymbol{\theta}$ such that $\boldsymbol{\theta}$ and $\boldsymbol{\rho}$ can be be uniquely identified when exact and sufficiently informative measurements of $\mathbf{u}(\boldsymbol{\theta}, t)$ and $\mathbf{v}(t)$ are provided. Additionally it is assumed that $\hat{\mathbf{g}}_n(\boldsymbol{\theta}, t)$ are given functions.

A natural selection for $\hat{\mathbf{g}}_n(\cdot, \cdot)$ would be harmonic functions where for linear systems this selection will result in a simple correspondence between $\mathbf{u}(\boldsymbol{\theta}, t)$ and $\mathbf{v}(t)$ for each $\hat{\mathbf{g}}_n(\boldsymbol{\theta}, t)$. In this work, the generation of periodic forces and the excitation of harmonic waves are mainly addressed. For this reason, we restrict ourselves to examples where harmonic functions are dealth with. Despite this restriction the general parameterisation developed so far is still valid for all the algorithms shown below. It is therefore assumed that the forces can be expressed as:

$$\mathbf{u}_d(t) = \mathbf{u}(\boldsymbol{\theta}_d, t) = \sum_{n=1}^{n_\theta} \boldsymbol{\theta}_{d,n} \cos n\omega t + \sum_{n=n_\theta+1}^{2n_\theta} \boldsymbol{\theta}_{d,n} \sin n\omega t. \tag{5}$$

Similarly, the input signals are written as:

$$\mathbf{v}(\boldsymbol{\rho}_d, t) = \sum_{n=1}^{n_\rho} \boldsymbol{\rho}_{d,n} \cos n\omega t + \sum_{n=n_\rho+1}^{2n_\rho} \boldsymbol{\rho}_{d,n} \sin n\omega t, \tag{5a}$$

where $\boldsymbol{\theta}_{d,n}(\boldsymbol{\rho}_{d,n})$ is the nth entry of the vector $\boldsymbol{\theta}_d$, $(\boldsymbol{\rho}_d)$.

In the last equation we chose the basis functions: $\hat{\mathbf{g}}_n(\boldsymbol{\theta}, t) = \boldsymbol{\theta}_{d,2n-1} \cos n\omega t$ and $\hat{\mathbf{g}}_{2n}(\boldsymbol{\theta}, t) = \boldsymbol{\theta}_{d,2n} \sin n\omega t$; $n = 1 \cdots 2n_\theta$. These functions are linear in $\boldsymbol{\theta}_d$, thus, the numerical search for a suitable excitation is greatly simplified.

A distance function relating the desired and obtained forces via their parameterisation is also defined:

$$\mathbf{J}(\boldsymbol{\theta}, \boldsymbol{\theta}_d) = \frac{\|\boldsymbol{\theta} - \boldsymbol{\theta}_d\|}{\|\boldsymbol{\theta}_d\|}. \tag{6}$$

The tuning process seeks to minimise $\mathbf{J}(\boldsymbol{\theta}, \boldsymbol{\theta}_d)$ by finding an appropriate vector of input signals $\mathbf{v}(t)$. Since $\mathbf{u}_d(t) \triangleq \mathbf{u}(\boldsymbol{\theta}_d, t)$ and $\mathbf{u}(\boldsymbol{\theta}, t)$ are single valued functions of $\boldsymbol{\theta}$, minimisation of equation (6) leads to a reduced distance between $\mathbf{u}_d(t)$ and $\mathbf{u}(\boldsymbol{\theta}, t)$ (in some vicinity of the optimum).

To assist in formulating the tuning algorithm a curve-fitting operator $\mathbf{F}(\cdot)$ providing $\hat{\boldsymbol{\theta}}$ which is an estimate of $\boldsymbol{\theta}$ is defined. In a formal representation one may write:

$$\hat{\boldsymbol{\theta}} = \mathbf{F}(\mathbf{u}(\boldsymbol{\theta}, t)), \qquad \hat{\boldsymbol{\rho}} = \mathbf{F}(\mathbf{v}(\boldsymbol{\rho}, t)), \tag{7, 7a}$$

where the expression $\hat{\boldsymbol{\rho}}_d \triangleq \mathbf{F}(\mathbf{v}_d(\boldsymbol{\rho}, t)) = \boldsymbol{\rho}_d$ is exact as it is not a measured quantity.

Substituting equation (7) into equation (6) gives

$$\mathbf{J}(\boldsymbol{\theta}, \boldsymbol{\theta}_d) = \frac{\|\hat{\boldsymbol{\theta}} - \boldsymbol{\theta}_d\|}{\|\boldsymbol{\theta}_d\|} = \frac{\|\mathbf{F}(\mathbf{u}(\boldsymbol{\theta}, t)) - \boldsymbol{\theta}_d\|}{\|\boldsymbol{\theta}_d\|}, \tag{8}$$

where $\|\cdot\|$ is user defined.

2.2. DESCRIPTIVE DEFINITION OF THE PROBLEM

In this section the mathematical problem which was defined above is described by a simplified (yet representative) schematic description of the proposed method. A typical laboratory set-up is illustrated in order to make the analytical and the descriptive arguments more tractable. In addition, some difficulties that typically arise in such a configuration are outlined.

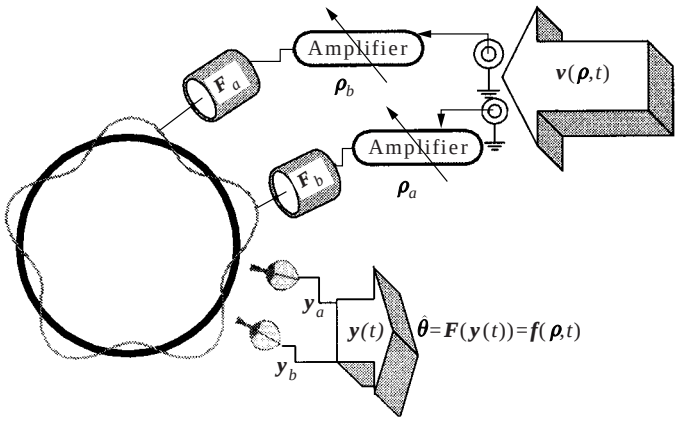

Figure 1. Experimental set-up showing the controlled signal $\mathbf{v}(\boldsymbol{\rho}, t)$, the curve-fitted parameter vector $\hat{\boldsymbol{\theta}}$ representing the adjusted response $\mathbf{y}(t)$.

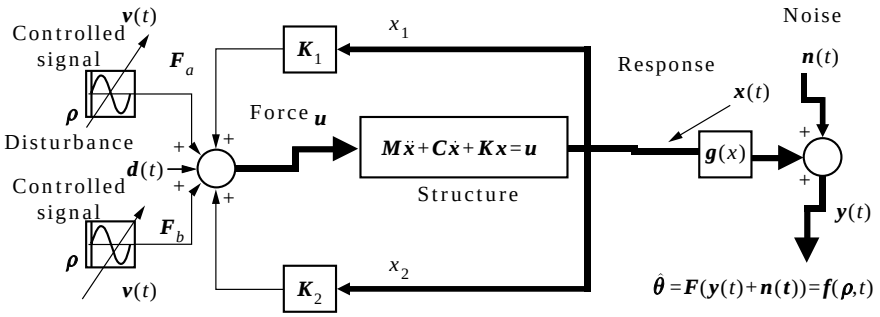

Figure 2. A schematic model of the experimental set-up showing the input signals $\mathbf{v}(t)$, controlled by the parameters $\boldsymbol{\rho}$ and the adjusted response $\mathbf{y}(t)$ (or force).

2.2.1. *An example for a force-tuned system*

The physical set-up of an existing experimental system controlled by the proposed algorithm is depicted in Figure 1. This system consists of two actuators and two controlled, response-related, variables (e.g., force or response).

The curve-fitted response, $\hat{\boldsymbol{\theta}} = \mathbf{F}(\cdot)$ (which may represent any quantity in the dynamic system, e.g., forces or displacement), is related to the various forces via equations (1, 2) and is fixed for a given $\boldsymbol{\rho}$. Realistically, the external forces include disturbances and are affected by inherent feedback [8]. In experiments where a vibrating structure is excited by means of electro-magnetic exciters, an inherent feedback may result in a combined non-linear dynamic system. The back electro-motive force (back-EMF) yields a reverse voltage, which creates the feedback in the shakers' windings. The diagram in Figure 2 describes a linear structure subject to external disturbances and to a non-linear feedback path.

The symbolic notation

$$\hat{\boldsymbol{\theta}} = \mathbf{F}(\mathbf{y}(t)) = \mathbf{f}(\boldsymbol{\rho}, t) \tag{9}$$

is used to demonstrate the implicit dependency of the curve-fitted parameter vector $\hat{\boldsymbol{\theta}}$ upon the controlled parameters $\boldsymbol{\rho}$ through the function $\mathbf{f}(\boldsymbol{\rho}, t)$.

The response vector $\mathbf{y}(t)$ (and hence $\hat{\boldsymbol{\theta}}$) is related to $\boldsymbol{\rho}$ via an unknown functional relation $\mathbf{f}(\boldsymbol{\rho}, t)$. This function represents a non-linear transformation between $\boldsymbol{\rho}$ and $\boldsymbol{\theta}$ which results from the non-linear force path and feedback. It is assumed that the non-linear part of the unknown model is concentrated in the feedback (vector) functions, $\mathbf{K}_1(\mathbf{x}(t))$, $\mathbf{K}_2(\mathbf{x}(t))$ appearing in equation (2).

The existence of feedback may lead (even a linear one) to some difficulties (e.g., singular behaviour of $\mathbf{f}(\boldsymbol{\rho}, t)$); this fact will be demonstrated later where different operating conditions of a vibrating system are analysed using the model represented by Figure 2. The proposed method is developed in section 3.

3. THE TUNING ALGORITHM AND THE INPUT SIGNAL OPTIMISATION PROCEDURE

A tuning algorithm which is considered successful must: (1) converge in a reasonably short time, and (2) should by no means exceed (diverge momentarily) from the allowed response limits.

The proposed algorithm attempts to fit a truncated polynomial model [16], which is in essence a truncated Volterra model. Consequently, the algorithm can cope with some non-linear behaviour and with non-linear internal feedback. This parameterisation is best suited for non-linear systems whose response frequency spectrum can be described by a parametric model. The automatic perturbation scheme that is used within the algorithm, requires smaller perturbations than any alternative direct approach (e.g., steepest descent) since it is constantly trying to enhance the measured signal to noise ratio rather than progress in the most favourable direction. A descriptive analysis of the capabilities and the properties of the algorithm are deferred to section 4.

3.1. THE FORCE AND RESPONSE TUNING METHOD—PRELIMINARY CONSIDERATIONS

In this section, the tuning method is developed as an adaptive (optimisation) process aimed at overcoming most of the difficulties that were outlined in section 2.

The problem of finding both the functional relationship in equation (2) (e.g., $\mathbf{f}(\boldsymbol{\rho}, t)$) and the vector of desired parameters, $\boldsymbol{\rho}$, is converted, using an appropriate parameterisation, into a set of locally-linearised equations. These equations are initially unknown and therefore a suitable process constructing both the unknown equations and the sought solution, $\boldsymbol{\rho}$, is employed. The process of finding an optimal input signal is divided into sub-problems for which a robust solution method is described. For this purpose, equation (9) relating the vector of desired variables, $\mathbf{F}(\mathbf{y}(t))$ and the (adjusted) parameters, $\boldsymbol{\rho}$ is used.

The goal of the tuning process is to find some $\hat{\boldsymbol{\rho}} = \boldsymbol{\rho}_d$ leading to $\hat{\boldsymbol{\theta}} = \boldsymbol{\theta}_d$ (in fact one obtains $\mathbf{F}(\mathbf{u}(\hat{\boldsymbol{\theta}}, t)) = \mathbf{F}(\mathbf{u}_d(t))$ and consequently $\mathbf{u}(\hat{\boldsymbol{\theta}}, t) = \mathbf{u}_d(t)$.

Mathematically one seeks a vector $\boldsymbol{\rho}_d$ leading to $\hat{\boldsymbol{\theta}} = \boldsymbol{\theta}_d$ which solves:

$$\hat{\boldsymbol{\theta}} = \mathbf{f}(\boldsymbol{\rho}_d, t). \tag{10}$$

Naturally, in real-world applications, equation (10) cannot be identically satisfied, thus a tolerance, ε and a convergence criterion need to be defined:

$$\boldsymbol{\rho}_d \in \{\underline{\boldsymbol{\rho}} \leqslant \boldsymbol{\rho} \leqslant \bar{\boldsymbol{\rho}}, \|\hat{\boldsymbol{\theta}}_d - \mathbf{f}(\boldsymbol{\rho}, t)\| \leqslant \varepsilon \|\hat{\boldsymbol{\theta}}_d\|\}. \tag{11}$$

Here $\underline{\boldsymbol{\rho}}$, $\bar{\boldsymbol{\rho}}$ are physical limits due to voltage limitation in the amplifiers or actuators. Also, ε is a user-selected tolerance.

Equations (10) or (11) suggests a numerical search algorithm attempting to achieve the goal stated in equation (11). This is done via an iterative search (minimisation) algorithm as described below.

3.1.1. *Development of the tuning algorithm*

Due to the unknown functional relation of $\boldsymbol{\theta}$ in $\boldsymbol{\rho}$, a probing (or identification) strategy needs to be employed. The proposed method is specifically designed to overcome many of the problems, which exist in a conventional direct approach.

The approach suggested can be viewed as a method for minimising the following error function:

$$J(\boldsymbol{\rho}) = \tfrac{1}{2}\mathbf{r}^T\mathbf{r}, \tag{12}$$

where the residual vector $\mathbf{r}$ is defined for any estimate of $\boldsymbol{\rho}$, as:

$$\mathbf{r} = \hat{\boldsymbol{\theta}}_d - \mathbf{f}(\boldsymbol{\rho}, t). \tag{13}$$

Here $\hat{\boldsymbol{\theta}}_d$ represents the desired force or response vector estimated by a curve-fitting procedure.

Ignoring temporarily the fact that the functional relationship, $\hat{\boldsymbol{\theta}} = \mathbf{f}(\boldsymbol{\rho}, t)$ is unknown, equation (10) is expanded in a truncated Taylor series:

$$\hat{\boldsymbol{\theta}} = \hat{\boldsymbol{\theta}}_0 + \Delta\hat{\boldsymbol{\theta}} = \mathbf{f}(\boldsymbol{\rho}_0, t) + \frac{\partial \mathbf{f}(\boldsymbol{\rho}_0, t)}{\partial \boldsymbol{\rho}^T} \Delta\boldsymbol{\rho} + O(\|\Delta\boldsymbol{\rho}\|^2), \tag{14}$$

where $O(\|\Delta\boldsymbol{\rho}\|^2)$ is the neglected residual.

Neglecting the second order residual term, one can write a simplified expression for equation (14):

$$\hat{\boldsymbol{\theta}} = \hat{\boldsymbol{\theta}}_0 + \mathbf{A}\Delta\boldsymbol{\rho}, \tag{15}$$

where

$$\mathbf{A} = \frac{\partial \mathbf{f}(\boldsymbol{\rho}_0, t)}{\partial \boldsymbol{\rho}^T}. \tag{16}$$

The goal is to achieve $\boldsymbol{\theta}_d = \hat{\boldsymbol{\theta}}_0$ (which corresponds to $\hat{\boldsymbol{\rho}}_d = \hat{\boldsymbol{\rho}}_0$), thus, defining a linearised set of equations:

$$\mathbf{A}\Delta\boldsymbol{\rho} \approx \boldsymbol{\theta}_d - \hat{\boldsymbol{\theta}}_0. \tag{17}$$

Knowledge of $\mathbf{A}$ and $\boldsymbol{\theta}_d - \hat{\boldsymbol{\theta}}_0$, would result in a one-step solution for this sub-task and consequently the updated parameters $\boldsymbol{\rho} = \boldsymbol{\rho}_0 + \Delta\boldsymbol{\rho}$ could be computed directly. Since neither $\mathbf{f}(\boldsymbol{\rho}, t)$ and hence nor $\mathbf{A}$ (which approximates $\mathbf{f}(\boldsymbol{\rho}, t)$) are known, an identification (probing) approach will be applied. Furthermore, $\mathbf{A} = \partial \mathbf{f}(\boldsymbol{\rho}_0, t)/\partial \boldsymbol{\rho}^T$ is a function of $\boldsymbol{\rho}_0$, thus, every new iteration in which $\boldsymbol{\rho}_0$ receives the value of the newly estimated $\boldsymbol{\rho}$ will yield a different model, $\mathbf{A}$, and would give rise to a locally linearised solution.

3.1.2. *Solution strategy*

The approach adopted in this work consists of two stages. In the first stage a robust variation of the Krylov subspace approach [13, 14] for solving equation (17) is being used providing an initial estimation of the model indicated by $\hat{\mathbf{A}}_0$. In the second stage, which is repeated until convergence, an optimal set of perturbation vectors is deduced from the updated model. The true model is perturbed around an operating point $\hat{\boldsymbol{\theta}}_0 = \mathbf{f}(\boldsymbol{\rho}_0, t)$ to yield:

$$\hat{\boldsymbol{\theta}} - \hat{\boldsymbol{\theta}}_0 \triangleq \Delta\boldsymbol{\theta} = \mathbf{f}(\boldsymbol{\rho}_0 + \Delta\boldsymbol{\rho}, t) - \mathbf{f}(\boldsymbol{\rho}_0, t). \tag{18}$$

Equation (18) demonstrates how one can replace $\mathbf{A}\Delta\boldsymbol{\rho}$ in equation (17) by two measurements: the first one at $\boldsymbol{\rho}_0$ and the second at $\boldsymbol{\rho}_0 + \Delta\boldsymbol{\rho}$. The generation of a set of probing vectors $(\Delta\boldsymbol{\rho})_k$ assists in obtaining an approximation for $\mathbf{A}$ and in progressing towards the required solution.

3.1.3. *The proposed algorithm*

Phase I: *generating an initial model*. The proposed method generates m orthonormal search directions, $\Delta\boldsymbol{\rho}_k = \boldsymbol{\rho}_{max}\mathbf{w}_k$, $k = 1 \cdots m$ via the Arnoldi procedure [13] creating a Krylov series [13]. During this process, a modified Gram–Schmidt process is carried out in order to assure the independence of the search directions and thus avoid numerical difficulties. The complete algorithm [22] is given in Appendix C.

The algorithm assumes some initial values, e.g., $\boldsymbol{\rho}_{max}$, $\boldsymbol{\rho}_0$, ε and $\boldsymbol{\theta}_0 = \mathbf{f}(\boldsymbol{\rho}_0, t)$ already described and consequently n measurements are performed

$$\hat{\boldsymbol{\theta}}_k = \mathbf{f}(\boldsymbol{\rho}_0 + \boldsymbol{\rho}_{max}\mathbf{w}_k, t), \qquad k = 1 \cdots n, \tag{19}$$

where $\mathbf{w}_k$ forms an orthonormal basis collected as columns of a matrix.

$$\mathbf{W} \triangleq [\mathbf{w}_1 \quad \mathbf{w}_2 \quad \cdots \quad \mathbf{w}_m]. \tag{20}$$

Similarly the fitted response parameter-vectors are gathered (see equation (18)) to yield:

$$\hat{\boldsymbol{\Theta}} \triangleq [\Delta\boldsymbol{\theta}_1 \quad \Delta\boldsymbol{\theta}_2 \quad \cdots \quad \Delta\boldsymbol{\theta}_m], \tag{21}$$

At this point one is able to use the linearised model of equation (17) to write

$$\mathbf{A}\boldsymbol{\rho}_{max}\mathbf{W} = \hat{\boldsymbol{\Theta}}, \tag{22}$$

from which one may obtain an estimate of the model

$$\hat{\mathbf{A}}_0 = \frac{1}{\boldsymbol{\rho}_{max}}\hat{\boldsymbol{\Theta}}\mathbf{W}^{-1}. \tag{23}$$

Here one can use the fact that $\mathbf{W}^{-1} = \mathbf{W}^T$ is orthonormal by construction (see Appendix C). In addition, the modified input vector $\boldsymbol{\rho}_0 + \Delta\boldsymbol{\rho}$ is deduced from

$$\Delta\boldsymbol{\rho} = \boldsymbol{\rho}_{max}\mathbf{W}\hat{\boldsymbol{\Theta}}^{-1}(\boldsymbol{\theta}_d - \boldsymbol{\theta}_0). \tag{24}$$

Phase II: *the main algorithm*. Given an estimate of the model $\hat{\mathbf{A}}_0$, one may form a SVD (singular values decomposition)

$$\hat{\mathbf{A}}_0 = \sum_{i=1}^{n} \hat{\sigma}_i\hat{\mathbf{u}}_i\hat{\mathbf{v}}_i^T. \tag{25}$$

Given the SVD, one is able to choose a set of perturbation vectors in the form:

$$\mathbf{w}_i = \frac{1}{\hat{\sigma}_i}\hat{\mathbf{v}}_i. \tag{26}$$

The set of perturbation-vectors is applied to the real system and each measurement is symbolised by (see equation (19)):

$$\hat{\boldsymbol{\theta}}_k = \mathbf{A}(\boldsymbol{\rho}_0 + \boldsymbol{\rho}_{max}\mathbf{w}_k) + \varepsilon_k, \tag{27}$$

where ε_k represents noise or model uncertainty.

Collecting all the measurements in one matrix, one may write, using equations (26) and (27),

$$\hat{\mathbf{\Theta}} = \boldsymbol{\rho}_{max}\mathbf{A}\hat{\mathbf{V}}\hat{\mathbf{\Sigma}}^{-1} + \mathbf{E}. \tag{28}$$

Here $\mathbf{E} = [\varepsilon_1 \ \varepsilon_2 \ \cdots \ \varepsilon_n]$.

Finally, temporarily neglecting the effect of noise, an updated approximation for the model is constructed

$$\hat{\mathbf{A}} = \frac{1}{\boldsymbol{\rho}_{max}}\hat{\mathbf{\Theta}}\hat{\mathbf{\Sigma}}\hat{\mathbf{V}}^{T}. \tag{29}$$

An increment towards the desired response can be computed according to equation (24)

$$\Delta\boldsymbol{\rho} = \boldsymbol{\rho}_{max}\hat{\mathbf{V}}\hat{\mathbf{\Sigma}}^{-1}\hat{\mathbf{\Theta}}^{-1}(\boldsymbol{\theta}_d - \hat{\boldsymbol{\theta}}_0). \tag{30}$$

If equation (11) is not satisfied, replace $\hat{\mathbf{A}}_0$ with $\hat{\mathbf{A}}$ and $\boldsymbol{\rho}_0$ with $\boldsymbol{\rho}_0 + \Delta\boldsymbol{\rho}$ and repeat equations (25) to (30)

Remark. The chosen perturbation in the ideal (noiseless) case would yield

$$\boldsymbol{\theta}_k = \boldsymbol{\rho}_{max}\mathbf{u}_k, \tag{31}$$

and therefore the numerical inversion of $\hat{\mathbf{\Theta}}$ (which needs to be performed in equation (30)) is optimally conditioned having a condition number equal to unity.

Proof: *optimality of perturbations without noise*. By orthogonality of the singular vectors $\mathbf{v}_i^T\mathbf{v}_k = \delta_{i,k}$,

$$\boldsymbol{\theta}_k = \hat{\mathbf{A}}_0\boldsymbol{\rho}_{max}\mathbf{w}_k = \sum_{i=1}^{n}\boldsymbol{\sigma}_i\mathbf{u}_i\mathbf{v}_i^T\boldsymbol{\rho}_{max}\frac{1}{\sigma_k}\mathbf{v}_k = \boldsymbol{\rho}_{max}\mathbf{u}_k. \tag{32}$$

Therefore $\hat{\mathbf{\Theta}} = \boldsymbol{\rho}_{max}[\mathbf{u}_1 \ \mathbf{u}_2 \ \cdots \ \mathbf{u}_n]$ which has perfect conditioning by construction of the SVD.

3.2. ROBUSTNESS AND CONVERGENCE ANALYSIS—SELECTION OF PERTURBATION SIZE

In this section the convergence properties of the proposed algorithm with respect to the signal to noise ratio are analysed. The difficulties, which arise due to singularity and due to measurement noise, affect the required perturbation step. This is shown explicitly in this section where the relationship between the degree of singularity of the system, the amount of measurement noise (model uncertainty) and the required perturbation step is developed. Expressed mathematically this relationship adds much understanding to the problem at hand and provides the motivation for the proposed method.

It is assumed that the system can be described via equation (17), e.g., by $\boldsymbol{\theta} = \mathbf{A}\boldsymbol{\rho}$. As will be shown in section 4, this relation is valid both for linear as well as some non-linear systems.

3.2.1. *Determination of the minimal step size for the direct approach*

An important question, which arises when studying any algorithm is whether stability can be guaranteed and under what circumstances will the algorithm converge. One usually wishes to induce the minimal amount of perturbation to the system and indeed the minimal required perturbation size that guarantees convergence is found below.

According to the algorithm which is proposed above, a set of orthogonal perturbation vectors, $\Delta\boldsymbol{\rho}_1, \Delta\boldsymbol{\rho}_2, \ldots$ is generated. All the generated vectors possess the same Euclidean length, ρ_{max} (the step-size), and the response to each of these input perturbations—$\hat{\boldsymbol{\theta}}_1, \hat{\boldsymbol{\theta}}_2, \ldots$ is estimated from measurements.

The estimated model of $\mathbf{A}$ indicated by $\hat{\mathbf{A}}_k$, is generated (in every iteration) from these data (in fact the inverse model is approximated implicitly).

Once the input signal (relative to the previous iteration) is updated using

$$(\hat{\boldsymbol{\rho}}_d)_i = (\hat{\boldsymbol{\rho}}_d)_{i-1} + (\Delta\hat{\boldsymbol{\rho}}_d)_{i-1} \tag{33}$$

and is applied to the system, an estimate of the desired response can be obtained:

$$(\hat{\boldsymbol{\theta}}_d)_i = \mathbf{A}(\hat{\boldsymbol{\rho}}_d)_{i-1} + \mathbf{A}(\Delta\hat{\boldsymbol{\rho}}_d)_{i-1} + \boldsymbol{\varepsilon} = (\hat{\boldsymbol{\theta}}_d)_{i-1} + \mathbf{A}((\hat{\boldsymbol{\rho}}_d)_i - (\hat{\boldsymbol{\rho}}_d)_{i-1})_i + \boldsymbol{\varepsilon}. \tag{34}$$

Here $\boldsymbol{\varepsilon}$ represents the uncertainty in the estimate (e.g., measurement noise).

Using equations (23, 27), one can form an estimate of the system's model:

$$\hat{\mathbf{A}}_k = (\hat{\boldsymbol{\Theta}} + \mathbf{E})\frac{1}{\boldsymbol{\rho}_{max}}\mathbf{W}^T, \tag{35}$$

where $\boldsymbol{\Theta} = [\hat{\boldsymbol{\theta}}_1 - (\hat{\boldsymbol{\theta}}_d)_{k-1}\ \hat{\boldsymbol{\theta}}_2 - (\hat{\boldsymbol{\theta}}_d)_{k-1}]$; $\mathbf{W} = [\Delta\boldsymbol{\rho}_1\ \Delta\boldsymbol{\rho}_2]$ and $\mathbf{E}$ is an error matrix representing the identification uncertainty which is directly related to $\boldsymbol{\varepsilon}$.

Using equation (35), one can estimate the required input signal for the $(k+1)$th iteration.

$$(\hat{\boldsymbol{\rho}}_d)_{k+1} = (\hat{\boldsymbol{\rho}}_d)_k + (\Delta\hat{\boldsymbol{\rho}}_d)_{k+1} = (\hat{\boldsymbol{\rho}})_k + \hat{\mathbf{A}}_k^{-1}(\boldsymbol{\theta}_d - (\hat{\boldsymbol{\theta}}_d)_k). \tag{36}$$

This input signal results in an estimate of the response $\boldsymbol{\theta}_d$:

$$(\hat{\boldsymbol{\theta}}_d)_{k+1} = \mathbf{A}(\hat{\boldsymbol{\rho}}_d)_{k+1} + \boldsymbol{\varepsilon} = \mathbf{A}(\hat{\boldsymbol{\rho}})_k + \mathbf{A}\hat{\mathbf{A}}_k^{-1}(\boldsymbol{\theta}_d - (\hat{\boldsymbol{\theta}}_d)_k) + \boldsymbol{\varepsilon} \tag{37}$$

or

$$(\hat{\boldsymbol{\theta}}_d)_{k+1} = (\hat{\boldsymbol{\theta}}_d)_k + \mathbf{A}\hat{\mathbf{A}}_k^{-1}(\boldsymbol{\theta}_d - (\hat{\boldsymbol{\theta}}_d)_k) + \boldsymbol{\varepsilon} \tag{38}$$

and rearranged,

$$(\hat{\boldsymbol{\theta}}_d)_{k+1} = [\mathbf{I} - \mathbf{A}\hat{\mathbf{A}}_k^{-1}](\hat{\boldsymbol{\theta}}_d)_k + \mathbf{A}\hat{\mathbf{A}}_k^{-1}\boldsymbol{\theta}_d + \boldsymbol{\varepsilon}. \tag{39}$$

Subtracting $\boldsymbol{\theta}_d$ from each side of the equality, one obtains an evolutionary equation for the deviation from the desired response $\{(\hat{\boldsymbol{\theta}}_d)_{k+1} - \boldsymbol{\theta}_d\}$:

$$(\{\hat{\boldsymbol{\theta}}_d)_{k+1} - \boldsymbol{\theta}_d\} = [\mathbf{I} - \mathbf{A}\hat{\mathbf{A}}_k^{-1}]\{(\hat{\boldsymbol{\theta}}_d)_{k+1} - \boldsymbol{\theta}_d\} + \boldsymbol{\varepsilon}. \tag{40}$$

This equation reveals much about the convergence properties of the direct and the proposed approaches. The algorithm will constantly improve (reduce the distance to the solution) at every iteration if;

$$(\sqrt{2}\kappa(\mathbf{A}) + 1)\frac{\|\mathbf{E}\|}{\underline{\sigma}(\mathbf{A})} \leqslant \boldsymbol{\rho}_{max}. \tag{41}$$

Proof: see Appendix B.

The stability analysis, which was conducted above, provides an expression for the required perturbation size. This expression is in fact a lower bound under which no convergence (i.e., divergence) will occur (on average). The solution of the inverse problem at hand requires a large perturbation step in order to achieve convergence. It can also be concluded that the deviation from the solution (error) is very sensitive to the least favourable direction dominated by $\sigma_{min}(\mathbf{A}) \equiv \underline{\sigma}(\mathbf{A})$.

Equation (41) demonstrates that the effective signal to noise ratio, $\|\mathbf{E}\|/\underline{\sigma}(\mathbf{A})$, is controlled by both the degree of singularity of the problem at hand and by the uncertainty (noise). The fact that the least favourable direction has such an important effect is not intuitive and has tremendous importance for identification and control algorithms.

3.2.2. *Determination of the minimal step for the proposed method*

In this case, the analysis follows immediately from equation (39) where the estimate from equation (29) is used to obtain:

$$\mathbf{I} - \mathbf{A}\hat{\mathbf{A}}_k^{-1} = \mathbf{A}\mathbf{A}^{-1} - \mathbf{A}\hat{\mathbf{V}}_k\hat{\boldsymbol{\Sigma}}_k\hat{\boldsymbol{\Theta}}_k^{-1} = \mathbf{A}\mathbf{A}^{-1} - \boldsymbol{\rho}_{max}\mathbf{A}\hat{\mathbf{V}}_k\hat{\boldsymbol{\Sigma}}_k^{-1}(\boldsymbol{\rho}_{max}\mathbf{A}\hat{\mathbf{V}}_k\hat{\boldsymbol{\Sigma}}_k^{-1} + \mathbf{E}_k). \tag{42}$$

Convergence is guaranteed if

$$\frac{\|(\hat{\boldsymbol{\theta}}_d)_{k+1} - \boldsymbol{\theta}_d\|}{\|(\hat{\boldsymbol{\theta}}_d)_k - \boldsymbol{\theta}_d\|} \leqslant 1, \tag{43}$$

which, according to equation (39) (and Appendix B), will occur if $\|\mathbf{I} - \mathbf{A}\hat{\mathbf{A}}_k^{-1}\| < 1$ or if

$$\|\mathbf{A}\mathbf{A}^{-1} - \boldsymbol{\rho}_{max}\mathbf{A}\hat{\mathbf{V}}_k\hat{\boldsymbol{\Sigma}}_k^{-1}(\boldsymbol{\rho}_{max}\mathbf{A}\hat{\mathbf{V}}_k\hat{\boldsymbol{\Sigma}}_k^{-1} + \mathbf{E}_k)\| \leqslant 1. \tag{44}$$

Performing some simplification one arrives at

$$\|\mathbf{A}\hat{\mathbf{V}}_k\hat{\boldsymbol{\Sigma}}_k^{-1}\|\left\|\hat{\boldsymbol{\Sigma}}_k\hat{\mathbf{V}}_k^T\mathbf{A}^{-1} - \left(\mathbf{A}\hat{\mathbf{V}}_k\hat{\boldsymbol{\Sigma}}_k^{-1} + \frac{1}{\boldsymbol{\rho}_{max}}\mathbf{E}_k\right)^{-1}\right\| \leqslant 1. \tag{45}$$

Finally, using the same procedure as shown in Appendix B, one obtains:

$$\boldsymbol{\rho}_{max} \geqslant \|\hat{\boldsymbol{\Sigma}}_k\hat{\mathbf{V}}_k^T\mathbf{A}^{-1}\|\,\|\mathbf{E}_k\|(1 + \sqrt{2}\,\|\hat{\boldsymbol{\Sigma}}_k\hat{\mathbf{V}}_k^T\mathbf{A}^{-1}\|\,\|\mathbf{A}\hat{\mathbf{V}}_k\hat{\boldsymbol{\Sigma}}_k^{-1}\|). \tag{46}$$

Convergence of the model, i.e., obtaining $\mathbf{A} = \hat{\mathbf{U}}_k\hat{\boldsymbol{\Sigma}}_k\hat{\mathbf{V}}_k^T$ would yield,

$$\|\hat{\boldsymbol{\Sigma}}_k\hat{\mathbf{V}}_k^T\mathbf{A}^{-1}\| = 1, \qquad \|\mathbf{A}\hat{\mathbf{V}}_k\hat{\boldsymbol{\Sigma}}_k^{-1}\| = 1. \tag{47}$$

It can therefore be deduced (substituting equation (47) into equation (46)) that the proposed algorithm requires an optimal (minimal) perturbation size of $\boldsymbol{\rho}_{max} \geqslant \|\mathbf{E}_k\|(1+\sqrt{2})$ to guarantee convergence. The proposed algorithm iteratively improves the estimate of the model and consequently the perturbation sequence will improve towards the ideal conditioning in equation (47).

3.2.3. *Advantages of the proposed algorithm*

In lieu of the above analysis, one can assess and describe the benefits of the proposed algorithm. In the proposed algorithm, one seeks to minimise the modelling error $\|\mathbf{A} - \hat{\mathbf{A}}_k\| = \|\mathbf{E}\| 1/\boldsymbol{\rho}_{max}$, by using the smallest possible perturbation size, $\boldsymbol{\rho}_{max}$ (minimal response levels are desired in non-destructive testing). The following two main points contribute to the ability of the algorithm to fulfil the abovementioned goals. (1) The input signals form an orthogonal basis, therefore, the numerical errors which may result from the inversion of the signal subspace $\mathbf{W}$ (see equation (23)) are prevented (this is because an orthogonal matrix has perfect numerical conditioning with respect to inversion). (2) The algorithm constantly perturbs the least favourable direction (in the parameters space), therefore, the signal to noise ratio is maximised and optimal convergence properties are obtained. This property is achieved by exploiting the information contained in the right singular vectors $\hat{\mathbf{V}}_k$ (computed in equation (29)). The singular vectors belonging to the smallest singular values span the null-space of the response and therefore contain the least favourable direction. By using a direct approach (rather than the proposed algorithm), there will be a need to increase the response levels so that the projection upon the weak direction (again in the parameter space) rises above the noise level. The proposed method, on the other hand, allows one to use a smaller perturbation size and consequently lower response levels are obtained. A more illustrative example is provided in a companion paper [23].

4. SOME ANTICIPATED DIFFICULTIES AND THE MODELLING APPROACH

In this section some of the anticipated difficulties arising during the tuning process are described in some detail. The model of the non-linear feedback terms under harmonic inputs is developed and its representation in a linearised form is explained.

4.1. THE EFFECT OF LINEAR FEEDBACK

In this part, the difficulties arising when the response level is high are discussed. High response levels are encountered, for example, when one seeks to excite a single vibration mode. This is usually achieved by choosing an excitation frequency close to the relevant natural frequency. When the level of motion is high, an electro-dynamic or electro-magnetic shaker creates a force which is greatly influenced by the large amplitudes [24]. Close to resonance, the force produced by a multi-exciter system might be dominated (due to the dependency upon the response) by the associate vibration mode-shape. In such cases it is therefore

difficult to produce a force which has components that are spatially orthogonal to the force caused by this effect.

The adjustment of the *response* near resonance, does not pose a severe problem when one seeks to produce a vibratory mode [11, 25], but the exact tuning of the *force* in such a regime may prove difficult [3]. This difficulty is due to reasons stated in reference [10] and for reasons stated below.

The displacement (velocity) dependent forces creates a feedback path [8] which is analysed here in the frequency domain.

The Fourier-transformed response of Ω (see equation (1)) can be expressed as:

$$\mathbf{X}(\omega) = \mathbf{H}(\omega)\mathbf{U}(\omega), \tag{48}$$

where $\mathbf{U}(\omega)$ is the applied force $\mathbf{X}(\omega)$ the response and $\mathbf{H}(\omega)$ the transfer matrix.

The displacement (or velocity) dependent force is shown schematically in Figure 3. Due to the (vector) static feedback having the gain-matrix $\mathbf{K}_f$ (see Figure 3), the actual force $\mathbf{U}(\omega)$ resulting from the input signal $\mathbf{V}(\omega)$ becomes:

$$\mathbf{U}(\omega) = \mathbf{V}(\omega) + \mathbf{K}_f\mathbf{X}(\omega). \tag{49}$$

Using equation (48) one can express the total applied force as:

$$\mathbf{U}(\omega) = \mathbf{V}(\omega) + \mathbf{K}_f\mathbf{H}(\omega)\mathbf{U}(\omega), \tag{50}$$

which shows how the exerted force is affected by the structural dynamics through the feedback term.

Introduction of equation (50) into equation (48), results in:

$$\mathbf{X}(\omega) = \mathbf{H}(\omega)(\mathbf{V}(\omega) + \mathbf{K}_f\mathbf{X}(\omega)), \tag{51}$$

or, rearranging

$$(\mathbf{I} - \mathbf{H}(\omega)\mathbf{K}_f)\mathbf{X}(\omega) = \mathbf{H}(\omega)\mathbf{V}(\omega). \tag{52}$$

Equations (48)–(52) allows one to analyse the effects of feedback when the response or the forces are to be adjusted.

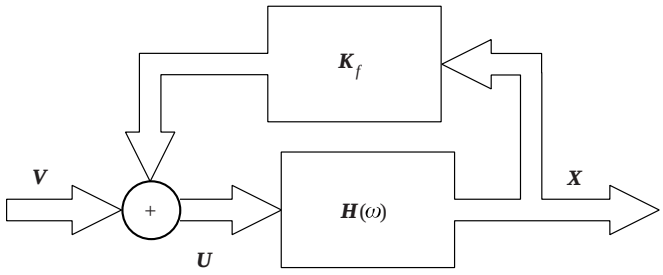

Figure 3. Block diagram of the force-feedback structure.

4.1.1. *The effect of feedback under high response levels*

When the excitation frequency ω is indeed close to one of the natural frequencies, ω_r, the frequency response matrix is dominated by the associated mode (the rth) and can be written as [9]:

$$\mathbf{H}(\omega) \approx \frac{\boldsymbol{\phi}_r \boldsymbol{\phi}_r^T}{\omega_r^2 - \omega^2 + \mathrm{i}\zeta_r \omega_r \omega} \tag{53}$$

where $\boldsymbol{\phi}_r$, ω_r, ζ_r are the mode shapes, modal damping and natural frequency respectively.

Clearly from equations (50) and (53) one can see that when ω is close to ω_r, both the force and the response are dominated by one of the eigenvectors. Consequently their spatial directionality is dictated, i.e.,

$$\mathbf{X}(\omega) \propto \boldsymbol{\phi}_r \qquad \mathbf{U}(\omega) \propto \mathbf{K}_f \boldsymbol{\phi}_r. \tag{54}$$

Any attempt to create response or force patterns considerably different from this spatial distribution, requires large input signals as this direction is greatly amplified by the small denominator of equation (53). In particular, when the desired force is almost orthogonal to this pattern, large $\mathbf{V}(\omega)$ (see equation (50)) is required in order to overcome the dominating $\mathbf{K}_f \mathbf{X}(\omega)$ term. This analysis is valid for any kind of feedback matrix, in particular for a diagonal one (i.e., the feedback is local to the actuator). When the feedback couples several degrees of freedom, one obtains further complications.

4.1.2. *Cross coupling due to feedback*

Due to feedback, a change in the force at one location could greatly influence the forces applied at other locations. This can be demonstrated by expressing the change in force due to a change in the control signal, $\mathbf{V}(\omega)$. From equation (50) one has:

$$\Delta\mathbf{U}(\omega) = \Delta\mathbf{V}(\omega) + \mathbf{K}_f \mathbf{H}(\omega) \Delta\mathbf{U}(\omega), \tag{55}$$

where $\Delta\mathbf{V}(\omega)$ represents changes in $\mathbf{V}(\omega)$ and $\Delta\mathbf{U}(\omega)$ the resulted change in $\mathbf{U}(\omega)$.

Rearranging equation (55), one obtains:

$$(\mathbf{I} - \mathbf{K}_f \mathbf{H}(\omega)) \Delta\mathbf{U}(\omega) = \Delta\mathbf{V}(\omega). \tag{56}$$

Very close to resonance $\omega_r \approx \omega$ which results in (see equation (53)):

$$\mathbf{H}(\omega) \approx \frac{-\mathrm{i}}{\zeta_r \omega_r^2} \boldsymbol{\phi}_r \boldsymbol{\phi}_r^T. \tag{57}$$

Therefore, equation (56), becomes:

$$\left(\mathbf{I} - \frac{\mathrm{i}}{\zeta_r \omega_r^2} \mathbf{K}_f \boldsymbol{\phi}_r \boldsymbol{\phi}_r^T\right) \Delta\mathbf{U}(\omega) = \Delta\mathbf{V}(\omega). \tag{58}$$

The coefficient matrix multiplying $\Delta\mathbf{U}(\omega)$ in equation (58) is no longer diagonal (as in the non-feedback case), therefore, a change of one force might influence other forces.

It is clear that for lightly damped structures where a high-gain feedback exists, the functional relationship between the force and the input signals is considerably modified. This equation is analysed in a companion paper [23] via several examples.

In this work the actual relationship between the input signal and the resulting forces is taken into account. In this way the algorithm automatically considers the effect of cross coupling between the various forces and thus the effect of feedback is automatically compensated.

Further complications can appear near resonance due the rank deficiency of the coefficients matrix in equation (58). This situation can occur when the damping is very small and may result in a rank one-coefficient matrix. The proposed algorithm handles the near-singular case by generating perturbations in the least dominant directions and thus obtaining the best possible estimate of the model.

4.1.3. *Non-linear force path and feedback, modelling and compensation*

In reality the force path may incorporate non-linear elements, e.g., electromagnetic devices. In this work, an attempt is made to accommodate a class of non-linear feedback functions and model them by a vector–Taylor series. Assuming that the function $\mathbf{K}_1(\cdot)$ can be developed in such a series (see reference [16], pp. 34–36), gives:

$$\mathbf{K}_1(\mathbf{x}(t)) \approx \sum_i \frac{\partial \mathbf{K}_1}{\partial \mathbf{x}_i(t)}\,\mathbf{x}_i(t) + \frac{1}{2}\sum_i \sum_j \frac{\partial^2 \mathbf{K}_1}{\partial \mathbf{x}_j(t)\,\partial \mathbf{x}_i(t)}\,\mathbf{x}_i(t)\mathbf{x}_j(t)$$

$$+ \frac{1}{6}\sum_i \sum_j \sum_k \frac{\partial^3 \mathbf{K}_1}{\partial \mathbf{x}_i(t)\,\partial \mathbf{x}_j(t)\,\partial \mathbf{x}_k(t)}\,\mathbf{x}_i(t)\mathbf{x}_j(t)\mathbf{x}_k(t) + \cdots. \tag{59}$$

The effect of the non-linear feedback can be cancelled in this case by subtracting the feedback functions, $\mathbf{K}_i(\cdot)$ from the force actually applied. The power terms greater than one are non-zero in equation (59) only when non-linear effects exist. Those terms can be cancelled by counteracting them in the controlled signal. Examining equation (2) one can show that a desired force vector $\mathbf{V}(t)$ will be achieved if one chooses v such that:

$$\sum_{k=1}^{P} \mathbf{F}_k(\boldsymbol{\theta}(v, t), t) = \mathbf{V}(t) - \sum_{k=1}^{P} \mathbf{K}_k(\mathbf{x}(t)) - \mathbf{d}(t). \tag{60}$$

The result of this force is essentially an exact linearisation of the system since the combined force becomes a linear function of $\mathbf{x}(t)$.

It is worth mentioning that in some cases, the disturbance, $\mathbf{d}(t)$, can be estimated and cancelled. For example, in rotating machines the unbalance can be estimated and cancelled by appropriate external forcing synchronous to rotation.

Successful tuning for which equation (60) holds, will yield (by substituting equation (60) into equation (2)):

$$\mathbf{u}(t) = \mathbf{V}(t) \tag{61}$$

Such a cancellation requires a complete identification of the coefficients in equation (59). This task can be formulated in a straightforward manner for harmonic input signals.

4.2. FORCE TUNING IN PRESENCE OF NON-LINEARITY UNDER HARMONIC EXCITATION

It can be shown that when the applied signals are sinusoidal, the power terms in equation (59) result in higher harmonics in the feedback terms (see also reference [16], chapter 5). Those terms can be identified and their unknown amplitudes could be added to the identified vector of unknown signal parameters, $\boldsymbol{\rho}$.

For example, in the dual shaker case (see Figures 1 and 2) one has, as in equation (5a):

$$\mathbf{v}(\rho, t) = \begin{pmatrix} \sum_{n=1}^{m} \boldsymbol{\rho}_{4n-3} \cos n\omega t + \sum_{n=m+1}^{2m} \boldsymbol{\rho}_{4n-2} \sin n\omega t \\ \sum_{n=1}^{m} \boldsymbol{\rho}_{4n-1} \cos n\omega t + \sum_{n=m+1}^{2m} \boldsymbol{\rho}_{4n} \sin n\omega t \end{pmatrix}$$

$$= \begin{pmatrix} \boldsymbol{\rho}_1 \cos \omega t + \cdots + \boldsymbol{\rho}_6 \sin 2\omega t + \cdots \\ \boldsymbol{\rho}_3 \cos \omega t + \cdots + \boldsymbol{\rho}_8 \sin 2\omega t + \cdots \end{pmatrix}, \tag{62}$$

where in this case one has $\boldsymbol{\rho} \in \Re^{8 \cdot m}$ and generally for tuning a system with n_s shakers and including n_h harmonics for every shaker there are $2n_s n_h$ parameters, $\boldsymbol{\rho}_i$.

A non-linear force path, which can be described by equation (59), can thus be handled under hamonic excitation. In this case the various harmonics should be identified (measured and curve-fitted) and then set to zero (in case those harmonics are to be suppressed). This strategy is demonstrated in section 5 and in a companion paper [23] for both simulated and for experimentally controlled structures.

4.2.1. *Representing the non-linear relation under harmonic excitation*

As shown above, the non-linear behaviour can be approximated as a truncated Taylor series, which gives rise to higher harmonics in the applied force $\mathbf{u}(t)$. Use is made of the curve-fitting operation in equation (7) to obtain equation (5) where the sine and a cosine coefficient for the ith measured force are found within the

fitted vector $\hat{\boldsymbol{\theta}}$ and are indicated by $\boldsymbol{\theta}^i_{sin}$ or $\boldsymbol{\theta}^i_{cos}$ for convenience. Using this parameterisation one can approximate equation (7) using equation (17) as:

$$\begin{Bmatrix} \theta^1_{cos} \\ \theta^1_{sin} \\ \vdots \\ \theta^{N_{nl}}_{sin} \end{Bmatrix} \cong \begin{bmatrix} A^{1,1}_{cos,cos} & A^{1,1}_{cos,sin} & \cdots & A^{1,N_{nl}}_{cos,sin} \\ \vdots & A^{1,1}_{sin,sin} & & A^{1,N_{nl}}_{sin,sin} \\ & & & \vdots \\ A^{N_{nl},1}_{sin,cos} & \cdots & & A^{N_{nl},N_{nl}}_{sin,sin} \end{bmatrix} \begin{Bmatrix} \rho^1_{cos} \\ \rho^1_{sin} \\ \vdots \\ \rho^{N_{nl}}_{cos} \end{Bmatrix}, \tag{63}$$

where $\theta^p_{cos} \cos p\omega t$ and $\theta^p_{sin} \sin n\omega t$ are the various harmonics for the pth measured response (or force).

Equation (59), represents a local approximation which is valid only at the specific operating point, therefore equation (63) represents a linearisation of the type:

$$A^{i,j}_{sin,sin} = \frac{\partial \theta^i_{sin}}{\partial \rho^j_{sin}}, \tag{64}$$

where *cos*, *sin* subscripts represent the sine–cosine coefficients and i, j superscript relate the ith harmonic in the response to the jth harmonic in the excitation.

The reader's attention is attracted to the similarity of the combined equations (59) and (63) to the so-called Volterra series. It can be shown [16, 17] that the single harmonic excitation part of the higher-order frequency response functions are in fact estimated. The approach presented has a distinct advantage over other Volterra-like identification schemes as the estimate is constantly updated until sufficient convergence is achieved. The converge is verified by comparison with the actually measured response of the system.

4.3. LINEAR VERSUS LINEARISED MODELS FOR THE TUNING AND IDENTIFICATION

As shown above, both the sine and cosine coefficients for every degree of freedom (and every harmonic in the non-linear case) are extracted. It is clear that there is a redundancy with respect to what is usually considered for linear systems. Indeed when the complete system consisting of the shakers and of a perfectly linear structure is considered, the minimal number of measurements required for identification of the frequency responses is (theoretically) equal to the number of actuators.

In the linear case, both amplitude and phase can be extracted from one measurement, as shown below. It is also shown here that this approach is not suitable for a linearised (non-linear) structure–shakers model and more measurements are required in order to identify a more general model. Although the assumption of an almost linear structure may lead to reasonably accurate identification, the resulting model is not sufficiently accurate for precise computation of the required forcing signals (for which a model inversion is requires).

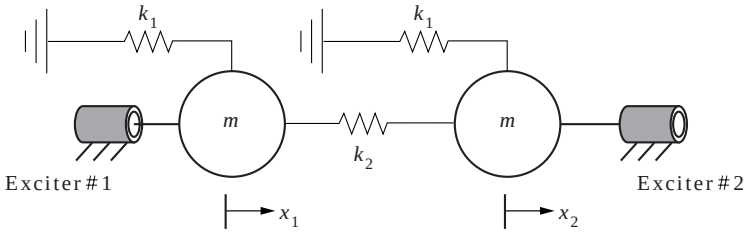

Figure 4. Nominal part of the simulated sytem.

A linear system represented by its complex frequency response function $H(\omega) = |H(\omega)|\, e^{i\phi}$ has the a steady state response of the form:

$$\mathbf{y} = \theta_{cos} \cos \omega t + \theta_{sin} \sin \omega t = |H(\omega)|(\rho_{cos} \cos(\omega t + \phi) + \rho_{sin} \sin(\omega t + \phi)), \quad (65)$$

where the input signal is $V = \rho_{cos} \cos \omega t + \rho_{sin} \sin \omega t$ while y is the output.

It can be shown (see Appendix A) that

$$\begin{pmatrix} \theta_{cos} \\ \theta_{sin} \end{pmatrix} \approx \begin{bmatrix} H_R & H_I \\ -H_I & H_R \end{bmatrix} \begin{pmatrix} \rho_{cos} \\ \rho_{sin} \end{pmatrix}. \quad (66)$$

Equations (65) and (66) assume that the identified system is perfectly linear while in fact a general linearised relation should be expressed as:

$$\begin{pmatrix} \Delta\theta_{cos} \\ \Delta\theta_{sin} \end{pmatrix} \approx \begin{bmatrix} \alpha_{11} & \alpha_{12} \\ \alpha_{21} & \alpha_{22} \end{bmatrix} \begin{pmatrix} \Delta\rho_{cos} \\ \Delta\rho_{sin} \end{pmatrix}. \quad (67)$$

A perfectly linear system can be identified by means of a single measurement where one chooses arbitrarily ρ_{cos}, ρ_{sin} and measures θ_{cos}, θ_{sin} to obtain:

$$H_R = \frac{\theta_{sin} + \theta_{cos}}{2\rho_{cos}}; \qquad H_I = \frac{\theta_{cos} - \theta_{sin}}{2\rho_{cos}}. \quad (68)$$

On the other hand, when a non-linear system is dealt with, the special structure of equation (66) is inappropriate and the more general equation (67) has to be used. In the linear case, the special relation in equation (66) is explained by the fact that the real and imaginary parts of the frequency response function are a Hilbert-transform pair [26].

For a non-linear system, four independent parameters (see equation (67), α_{ij} $i, j = 1, \ldots, 2$) need to be identified, thus, at least two independent measurements (two independent ρ_{cos}, ρ_{sin} combinations should be used) are required (to obtain a scalar linearised model).

This idea is further developed for a non-linear multi-exciter model and is in fact employed in equation (63). An interesting feature of the modelling used in equation (63) is that the structure of equation (66) can be extended to systems described by Volterra series.

A multi-shaker response system will have similar properties when the input-signal output-force are considered. In this case, 2 by 2 blocks having similar

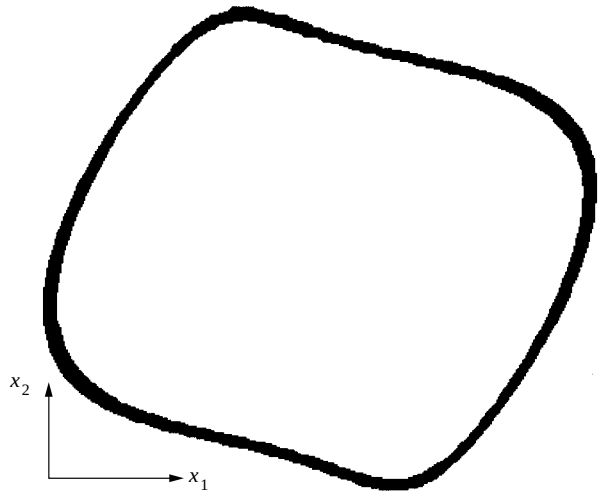

Figure 5. Tuned steady state response using one harmonic in the excitation.

structure to equations (66) and (67) can be identified (see Appendix A). This special structure will be demonstrated in the example provided in section 5. Any deviation from this structure (of equation (66)) implies that some (asymmetric) non-linearity exists, as is demonstrated by simulation in section 5 and experimentally in an additional work [23].

5. ILLUSTRATIVE EXAMPLE

In this section the proposed algorithm is applied to a simulated system. The results are plotted and briefly discussed. The example shown here is based on a simulation of a non-linear system. More detailed examples and experimental case studies are deferred (due to lack of space) to a companion paper [23].

The nominal system (without the non-linear feedback terms) is depicted in Figure 4.

The simulated system can be described by equation (1) where $\mathbf{M}, \mathbf{K}$ are determined from Figure 4 using the values of $m = 0{\cdot}3$, $k_1 = 8{\cdot}1$, $k_2 = 35{\cdot}8$ and $\mathbf{C} = 0{\cdot}2\mathbf{M} + 0{\cdot}003\mathbf{K}$. The forcing term $\mathbf{u}(t)$ is defined according to equation (2) in addition to some non-linear feedback terms.

TABLE 1

A-*matrix for case* 1 (*see equation* (37))

0.5528	0.1633	−0.4279	0.1603
−0·1387	0·5040	−0·1406	−0·4770
−0·4250	0·1574	0·5552	0·1612
−0·1415	−0·4725	−0·1382	0·5071

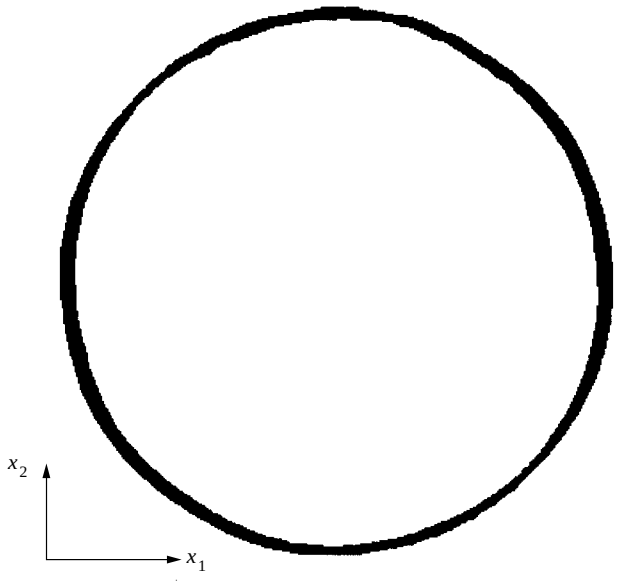

Figure 6. Tuned steady state response using six harmonics in the excitation.

The equation of motion of the structure is:

$$\mathbf{M}\ddot{\mathbf{x}}(t) + \mathbf{C}\dot{\mathbf{x}}(t) + \mathbf{K}\mathbf{x}(t) = -\mathbf{x}(t) - 3\mathbf{x}^3(t) + \sum_{k=1}^{NH} \boldsymbol{\rho}_k^{sin} \sin(k\omega t) + \boldsymbol{\rho}_k^{cos} \cos(k\omega t), \tag{69}$$

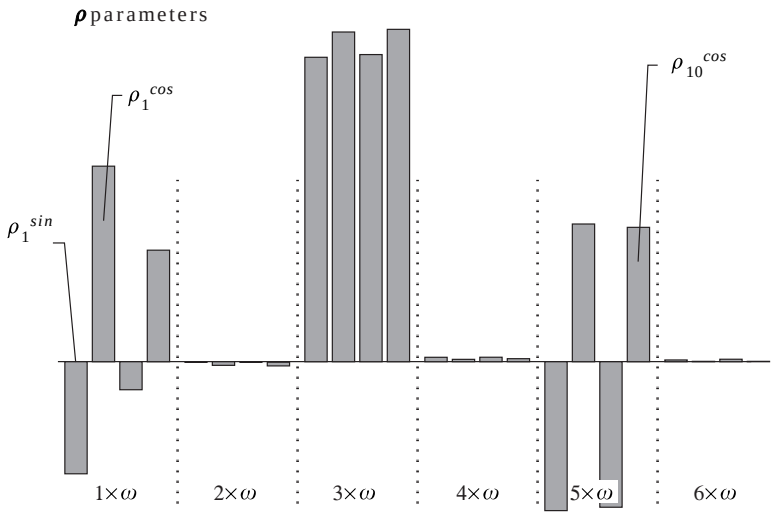

Figure 7. Tuned amplitudes for the various harmonics.

where $\boldsymbol{\rho}_k^{sin}$, $\boldsymbol{\rho}_k^{cos} \in \Re^{2\times 1}$ are tuned in order to achieve the desired response, expressed as:

$$\boldsymbol{\theta}_1^{sin} = \begin{pmatrix} 0{\cdot}2 \\ 0 \end{pmatrix}, \qquad \boldsymbol{\theta}_1^{cos} = \begin{pmatrix} 0 \\ 0{\cdot}2 \end{pmatrix}, \qquad \boldsymbol{\theta}_k^{p} = 0 \;\forall k > 1, \qquad p \in \{\sin, \cos\}. \tag{70}$$

5.1. CASE 1: USING ONE HARMONIC IN THE INPUT

In the first simulation run, only one harmonic was used in the forcing signal ($NH = 1$). The required response plotted in the x_1, x_2 plane would ideally look like a perfect circle (this can be deduced from equation (70)). Due to the non-linear behaviour, higher harmonics were excited and the results shown in Figure 5 indeed indicate a distortion.

The identified matrix **A** is given in Table 1. This matrix shows that equation (66) does not hold (or equation (A(6)) and the more general equation (67) is required for the 2×2 blocks. For this case full convergence was achieved for the first harmonic of the response, but the effect of the higher harmonics obviously affect the results and so an imperfect result was obtained.

5.2. CASE 2: USING SIX HARMONICS

An additional simulation was conducted for the same system where in this case six harmonics were tuned. The results are depicted in Figure 6. This figure clearly shows an obvious improvement over the single harmonic case (Figure 5). The algorithm converged in both cases in three steps, but due to the larger number of parameters, case 2 required a larger number of perturbation runs. The tuned parameters are shown in Figure 7. In this figure the importance of the odd harmonics and in particular the third one is clearly shown and the effectiveness of the proposed algorithm in cancelling the non-linear effects was demonstrated. An additional study, which includes several experimental cases, is shown in a companion paper [23].

6. CONCLUSIONS

In this paper a novel approach for tuning a multi-exciter system is introduced. The method takes into account various difficulties, such as, model uncertainty, feedback, singular models and inferior signal to noise ratios. By creating a high order model, which describes a non-linear system subject to harmonic forcing, the method adaptively tunes the forcing signal until the desired excitation or response is achieved. The conditions under which convergence of the algorithm is guaranteed are developed in this paper. The algorithm attempts to maximise the effective signal to noise ratio and allows for smaller perturbations and lower response levels while still guaranteeing convergence. A simulation shown in this paper illustrates the capabilities of the proposed algorithm in exact tuning of a desired response and in cancellation of non-linear effects. The presented method has further potential in other types of inverse problems where an adaptive approach is required in order to maximise the amount of extracted information with respect to noise and uncertainty.

REFERENCES

1. P. Schmiechen 1997 *PhD Thesis*, *Imperial College London*. Travelling-wave-speed instability.
2. C. W. Lee and J. Young-Don 1993 *Mechanical Systems and Signal Processing* **7**, 57–74. Theory of excitation methods and estimation of frequency response functions in complex modal testing of rotating machinery.
3. I. Bucher *et al*. 1995 *The Royal Aeronautical Society Forum*, *Manchester*, June. Automatic force or response adjustment in a multi-shaker excitation system using a non-linear optimisation approach.
4. I. Bucher *et al*. 1995 To be presented in Society Francais Des Mechanicies, *Acoustical & Vibratory Surveillance*, *Methods & Diagnostic Techniques*, *Paris*, October. Directional and multi-dimensional spectrograms and Campbell diagrams: a diagnostic and surveillance tool for rotating machinery.
5. P. Schmiechen 1995 *ASME Winter Annual Meeting*, *Boston*, *MA*. Excitation of travelling waves.
6. Y. S. Cho, S. B. Kim, E. L. Hixson and E. J. Powers 1993 *IEEE Transactions on Acoustics*, *Speech and Signal Processing* **40**, 1029–1040. A digital technique to estimate second order distortion using higher order coherence spectra.
7. G. Genta 1988 *Journal of Sound and Vibration* **124**, 27–53. Whirling of unsymmetrical rotors: A finite element approach based on complex co-ordinates.
8. W. M. To and D. J. Ewins 1991 *Mechanical Systems and Signal Processing* **5**, 305–316. A closed-loop model for single/multi-shaker modal testing.
9. D. J. Ewins 1984 *Modal Testing*. Letchworth: Research Studies Press.
10. I. Bucher and S. Braun 1997 *ASME Transactions*: *Journal of Applied Mechanics* **64,** 97–105. Braun, left-eigenvectors: extraction from measurements and physical interpretation.
11. E. Breitbach 1973 *Proceedings of the* 3*rd Euro Testing Symposium*. A semi-automatic modal survey test technique for complex aircraft and space structures.
12. Brite 1996 Final report of a European community funded project, no. BE5464. Modal analysis of rotating structures.
13. Y. Saad and M. H. Schultz 1986 *Siam Journal on Scientific and Statistical Computing* **7**, 856–869. GMRES: a generalized minimal residual algorithm for solving non-symmetric linear systems.
14. O. Axelsson 1988 *Linear Algebra Applications* **29**, 1–16. Conjugated gradient type methods for unsymmetric and inconsistent systems of linear equations.
15. R. Fletcher 1987 *Practical Methods of Optimization*. New York: Wiley-Interscience; second edition.
16. W. J. Rugh 1981 *Nonlinear System Theory—the Volterra/Wiener Approach*. Baltimore, MA: John Hopkins University Press.
17. S. A. Billings and M. I. Yusof 1996 *International Journal of Control* **65,** 589–618. Decomposition of generalized frequency response functions for nonlinear systems using symbolic computation.
18. D. M. Storer and G. R. Tomlinson 1993 *Mechanical Systems and Signal Processing* **7**. Recent developments in the measurement and interpretation of higher order transfer functions from non-linear structures.
19. J. C. Peyton Jones and S. A. Billings 1989 *International Journal of Control* **50,** 1925–1940. Recursive algorithm for computing the frequency response of a class of non-linear difference equation models.
20. J. Bendat 1990 *Nonlinear System Analysis and Identification from Random Data*. New York: John Wiley & Sons.
21. M. Schetzen 1980 *The Volterra and Wiener Theories of Nonlinear Systems*. New York: John Wiley & Sons.
22. C. T. Kelly 1995 *Iterative Methods for Linear and Nonlinear Equations*. SIAM Philadelphia.

23. I. BUCHER 1998 *Journal of Sound and Vibration*, in preparation. On the cancellation of coupled harmonic distortions in a multi degrees of freedom system—examples and experimental case-studies.
24. H. WOODSON and J. R. MELCHER 1968 *Electromechanical Dynamics*. London: Wiley; parts 1, 2.
25. P. A. ATKINS, G. R. TOMLINSON and J. R. WRIGHT 1994 *International Modal Analysis Conference*, *Nashville*, TN. Force appropriation of simple non-linear systems.
26. A. B. PIRARD 1989 *The Physics of Vibration*. Cambridge University Press.
27. A. BJÖRCK 1996 *Numerical Methods for Least Squares Problems*. SIAM Philadelphia.

APPENDIX A

In this appendix the special structure of a linear system appearing in the identified matrix, **A**, is developed. This structure is no longer suitable for non-linear (and for linearised) structures thus a need for a larger number of perturbations is illustrated.

First analyse a single-input single-output linear system where the input (voltage) is: $V = \rho_1 \cos \omega t + \rho_2 \sin \omega t$ and the resulted response is $F = \theta_1 \cos \omega t + \theta_2 \sin \omega t$. This linear system can be described by means of its transfer $H_a = |H| \, e^{j\phi}$, therefore, in this case, the output is related to the input (voltage) by:

$$\theta = |H|(\rho_1 \cos(\omega t + \phi) + \rho_2 \sin(\omega t + \phi)) \tag{A1}$$

or

$$\theta = |H|((\rho_1 \cos \omega t + \rho_2 \sin \omega t) \cos \phi + (\rho_2 \cos \omega t - \rho_1 \sin \omega t) \sin \phi). \tag{A2}$$

Making use of the identities, $H_R = |H| \cos \phi$; $H_I = |H| \sin \phi$, one has

$$\theta = (H_R \rho_1 + H_I \rho_2) \cos \omega t + (H_R \rho_2 - H_I \rho_1) \sin \omega t. \tag{A3}$$

Hence,

$$\theta_1 = (H_R \rho_1 + H_I \rho_2); \qquad \theta_2 = (H_R \rho_2 - H_I \rho_1). \tag{A4}$$

From equation (A4) one can finally observe that:

$$\frac{\partial \theta_1}{\partial \rho_1} = H_R = \frac{\partial \theta_2}{\partial \rho_2} \qquad \frac{\partial \theta_1}{\partial \rho_2} = H_I = -\frac{\partial \theta_2}{\partial \rho_1}. \tag{A5}$$

Developing a small perturbation of the response in a truncated Taylor series gives:

$$\Delta F \approx F_{cos} \cos \omega t + F_{sin} \sin \omega t \approx \left(\frac{\partial \theta_1}{\partial \rho_1} \Delta \rho_1 + \frac{\partial \theta_1}{\partial \rho_2} \Delta \rho_2 \right) \cos \omega t$$

$$+ \left(\frac{\partial \theta_2}{\partial \rho_1} \Delta \rho_1 + \frac{\partial \theta_2}{\partial \rho_2} \Delta \rho_2 \right) \sin \omega t, \tag{A6}$$

$$\begin{pmatrix} F_{cos} \\ F_{sin} \end{pmatrix} \approx \begin{bmatrix} \dfrac{\partial \theta_{cos}}{\partial \rho_{cos}} & \dfrac{\partial \theta_{cos}}{\partial \rho_{sin}} \\ \dfrac{\partial \theta_{sin}}{\partial \rho_{cos}} & \dfrac{\partial \theta_{sin}}{\partial \rho_{sin}} \end{bmatrix} \begin{pmatrix} \Delta \rho_{cos} \\ \Delta \rho_{sin} \end{pmatrix}. \tag{A7}$$

Finally substituting equation (A5) into equation (A6) and comparing terms gives equation (66)

$$\begin{pmatrix} F_{cos} \\ F_{sin} \end{pmatrix} \approx \begin{bmatrix} H_R & H_I \\ -H_I & H_R \end{bmatrix} \begin{pmatrix} \Delta \rho_{cos} \\ \Delta \rho_{sin} \end{pmatrix}. \tag{A8}$$

Equation (A6) can be extended for the dual-exciter dual-response linear system depicted in Figure 1.

$$\begin{pmatrix} \theta^a_{cos} \\ \theta^a_{sin} \\ \theta^b_{cos} \\ \theta^b_{sin} \end{pmatrix} = \begin{bmatrix} H^{a,a}_R & H^{a,a}_I & H^{a,b}_R & H^{a,b}_I \\ -H^{a,a}_I & H^{a,a}_R & -H^{a,b}_I & H^{a,b}_R \\ H^{b,a}_R & H^{b,a}_I & H^{b,b}_R & H^{b,b}_I \\ -H^{b,a}_I & H^{b,a}_R & -H^{b,b}_I & H^{b,b}_R \end{bmatrix} \begin{pmatrix} \rho^a_{cos} \\ \rho^a_{sin} \\ \rho^b_{cos} \\ \rho^b_{sin} \end{pmatrix}, \tag{A9}$$

where clearly for this case

$$A^{i,j}_{cos,cos} = \frac{\partial \theta^i_{cos}}{\partial \rho^j_{cos}} = H^{i,j}_R \qquad \text{and} \qquad A^{i,j}_{cos,sin} = \frac{\partial \theta^i_{cos}}{\partial \rho^j_{sin}} = H^{i,j}_I \qquad \text{etc.}$$

It is clear that columns 2 and 4, for example, can be calculated from columns 1 and 3. Therefore, in this case only two input vectors (of input-voltage signals) should suffice. Here $H_{R_{ab}} + jH_{I_{ab}} = \theta_a/\rho_b$: the transfer function between ρ_b and θ_a.

APPENDIX B

In this appendix equation (41) is formally proved. In order to assure stability and convergence it is required (given equation (40)) that:

$$\frac{\|(\hat{\boldsymbol{\theta}}_d)_{k+1} - \boldsymbol{\theta}_d\|}{\|(\hat{\boldsymbol{\theta}}_d)_k - \boldsymbol{\theta}_d\|} \leqslant 1. \tag{B1}$$

Hence, it is required

$$\|\mathbf{I} - \mathbf{A}\hat{\mathbf{A}}_k^{-1}\| < 1 \tag{B2}$$

or

$$\|\mathbf{A}\mathbf{A}^{-1} - \mathbf{A}\hat{\mathbf{A}}_k^{-1}\| < 1. \tag{B3}$$

Using the results from reference [27, equations (1.4.9) and (1.4.12)] gives

$$\|\mathbf{A}\|\|\mathbf{A}^{-1} - \hat{\mathbf{A}}_k^{-1}\| \leqslant \|\mathbf{A}\|\|\mathbf{A}^{-1}\|^2 \frac{\sqrt{2}\|\mathbf{A} - \hat{\mathbf{A}}_k\|}{1 - \|\mathbf{A}^{-1}\|\|\mathbf{A} - \hat{\mathbf{A}}_k\|} \leqslant 1. \tag{B4}$$

From equation (35) one can deduce that

$$\|\mathbf{A} - \hat{\mathbf{A}}_k\| = \|\mathbf{E}\| \frac{1}{\boldsymbol{\rho}_{max}} \tag{B5}$$

and therefore equation (B4) becomes

$$\frac{\kappa(\mathbf{A})}{\underline{\sigma}(\mathbf{A})} \frac{\sqrt{2}\|\mathbf{E}\| \frac{1}{\boldsymbol{\rho}_{max}}}{1 - \frac{\|\mathbf{E}\|}{\boldsymbol{\rho}_{max}\underline{\sigma}(\mathbf{A})}} \leqslant 1. \tag{B6}$$

The perturbation size, $\boldsymbol{\rho}_{max}$, which guarantees stability of the proposed algorithm, is bounded by:

$$\frac{\kappa(\mathbf{A})}{\underline{\sigma}(\mathbf{A})} \frac{\sqrt{2}\|\mathbf{E}\|}{1 - \frac{\|\mathbf{E}\|}{\boldsymbol{\rho}_{max}\underline{\boldsymbol{\sigma}}(\mathbf{A})}} \leqslant \boldsymbol{\rho}_{max}. \tag{B7}$$

Assuming that $1 > \|\mathbf{E}\|/\boldsymbol{\rho}_{max}\underline{\boldsymbol{\sigma}}(\mathbf{A})$ [27, equation (1.4.9)] one finally obtains:

$$(\sqrt{2}\kappa(\mathbf{A}) + 1) \frac{\|\mathbf{E}\|}{\underline{\boldsymbol{\sigma}}(\mathbf{A})} \leqslant \boldsymbol{\rho}_{max}. \tag{B8}$$

APPENDIX C

In this appendix, the initialisation part of the algorithm is provided. This part is carried out when there is no initial model therefore the perturbation sequence needs to be constructed from scratch.

Part I: probing, generating a set of measurements and a basis for the solution using the Arnoldi process type of procedure.

Form basis (Indirect Identification)

Given: $\boldsymbol{\rho}_{max}, \boldsymbol{\rho}_0, \boldsymbol{\epsilon}$

STEP I: compute $\boldsymbol{\theta}_0 = \mathbf{f}(\boldsymbol{\rho}_0, \omega t)$ take initial measurement

$$\mathbf{v}_1 = \boldsymbol{\theta}_d - \boldsymbol{\theta}_0, \quad \mathbf{w}_1 = \frac{\mathbf{v}_1}{\|\mathbf{v}_1\|}, \qquad k = 1$$

STEP II: **A: while** $\|\boldsymbol{\theta}_d - \boldsymbol{\theta}_{k-1}\| \leqslant \epsilon\boldsymbol{\theta}_d$ **and** $k \leqslant m$

$\boldsymbol{\theta}_k = \mathbf{f}(\boldsymbol{\rho}_0 + \boldsymbol{\rho}_{max}\mathbf{w}_k, \omega t)$ take one measurement.

$\mathbf{v}_{k+1} = \boldsymbol{\theta}_d - \boldsymbol{\theta}_k$

B: repeat $q = 1 \cdots k - 1$ orthogonalisation.

$$\mathbf{v}_{k+1} \leftarrow \mathbf{v}_{k+1} - (\mathbf{v}_{k+1}^T\mathbf{w}_q)\mathbf{w}_q$$

B: end

$$\mathbf{w}_{k+1} = \frac{\mathbf{v}_{k+1}}{\|\mathbf{v}_{k+1}\|}, \qquad \Delta\boldsymbol{\theta}_k = \boldsymbol{\theta}_k - \boldsymbol{\theta}_0, \qquad k = k + 1$$

A: end